

Correlated magnetic reversal in periodic stripe patterns

Katharina Theis-Bröhl,* Boris P. Toperverg,† Vincent Leiner, Andreas Westphalen, and Hartmut Zabel
Department of Physics, Ruhr-University Bochum, 44780 Bochum, Germany

Jeffrey McCord
*Leibniz Institute for Solid State and Materials Research Dresden, Institute for Metallic Materials,
 Helmholtzstr. 20, D-01169 Dresden, Germany*

Karsten Rott and Hubert Brückl
Department of Physics, University Bielefeld, Universitätsstr. 25, 33615 Bielefeld, Germany
 (Received 19 November 2004; published 19 January 2005)

The magnetization reversal in a periodic magnetic stripe array has been studied with a combination of direct and reciprocal space methods: Kerr microscopy and polarized neutron scattering. Kerr images show that during magnetization reversal over a considerable magnetic-field range a ripple domain state occurs in the stripes with magnetization components perpendicular to the stripes. Quantitative analysis of polarized neutron specular reflection, Bragg diffraction, and off-specular diffuse scattering provides a detailed picture of the mean magnetization direction in the ripple domains as well as longitudinal and transverse fluctuations, and reveals a strong correlation of those components over a number of stripes.

DOI: 10.1103/PhysRevB.71.020403

PACS number(s): 75.75.+a, 61.12.Ha, 75.60.Ej

The magnetization reversal of individual magnetic elements within a periodic array may or may not affect the behavior of its neighbors depending on the range of the stray fields emanating from its edges. Understanding and controlling interactions between neighboring elements is of high fundamental and technological relevance for magneto-electronic applications. However, experimental analysis of correlation effects is not an easy task. We have chosen polarized neutron reflectivity (PNR) to characterize the magnetization reversal and to unravel simultaneously the strength and range of magnetic correlations. PNR is a particularly well-suited experimental tool for this task as it is magnetically sensitive, allows to determine the mean vectorial magnetization direction, and, in particular, contains all required information on fluctuation and correlation effects.¹⁻⁶ Recently polarized neutron reflectivity and scattering has also successfully been applied to patterned magnetic films prepared by lithographic means.⁷⁻⁹ We have investigated the magnetization reversal of a magnetic stripe array via a combination of neutron scattering and Kerr microscopy. The stripes exhibit ripplelike domain patterns over a wide magnetic field range, giving rise to *intra*- and *inter*stripe correlations effects. The detailed quantitative analysis of the neutron data yielding information on longitudinal and transverse magnetization fluctuations considerably extends the information achievable by photon- or electron-based imaging techniques.

The main goal of the present study is to follow the evolution of the magnetization distribution in a stripe pattern with an induced uniaxial magnetic shape anisotropy as a function of field. Such systems are not only interesting in view of their potentials for nanoelectronics, but also due to fundamental problems of the interplay between induced and self-ordering in quasi-two-dimensional (quasi-2D) magnetic systems. In this Communication we demonstrate that the fundamental problems of the interplay between induced and self-ordering in quasi-2D magnetic systems can be success-

fully addressed by combining the benefits of magneto-optic Kerr effect (MOKE) and Kerr microscopy (KM) with results from PNR. While KM provides direct-space images of magnetic domains, PNR probes both the parallel and the perpendicular components of the magnetization distribution in the Fourier space.

We investigated the magnetization reversal of a lateral array consisting of polycrystalline stripes with a layer stack of 3 nm V, 76 nm $\text{Co}_{0.7}\text{Fe}_{0.3}$, and 3 nm of Al for protection, deposited on an $\text{Al}_2\text{O}_3(1102)$ substrate with a 5-nm-thick Ta buffer layer. The stripes have a width of 2.4 μm and a grating period of 3 μm , thus the anisotropy of the stripes is dominated by shape anisotropy. In comparative measurements on a continuous film, no anisotropy was visible by regular MOKE magnetometry.

Neutron-scattering experiments were carried out with the ADAM reflectometer of the Institut Laue-Langevin, Grenoble, France.¹⁰ The measurements were performed with a fixed neutron wavelength, $\lambda=0.441$ nm. A magnetic field was applied perpendicular to the scattering plane and parallel to the stripes. If not explicitly defined otherwise, the terms parallel and perpendicular refer to the direction of the stripes in the film plane, whereas longitudinal and transverse refer to the mean magnetization direction.

In the easy-axis configuration one can expect a “classical” remagnetization scenario, which implies homogeneous magnetization along the stripes below the coercive field H_c and an almost instantaneous flip of the magnetization into the field direction at H_c .⁸ Instead, with KM a ripplelike multidomain structure was observed already close to remanence, far below H_c , as shown in Fig. 1(a). The contrast between neighboring domains is produced by magnetization directions, which are tilted away to the left and to the right relative to the net magnetization.¹⁴ Increasing the magnetic field does not affect the domain size or orientation. At H_c [Fig. 1(b)], the magnetization in some of the stripes suddenly alters its

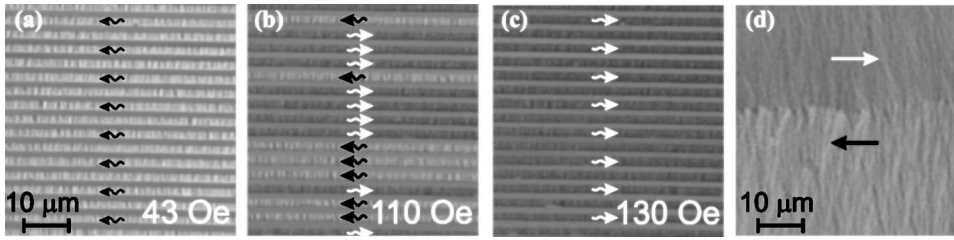


FIG. 1. Kerr microscopy images taken below H_c (a), at H_c (b), and above H_c (c) with the magnetic field aligned parallel to the stripes. The plane of incidence results in a top-down magneto-optical sensitivity axis perpendicular to the stripes. The curly arrows indicate the mean magnetization direction as well as the presence of ripple domains. (d) Kerr microscopy image taken at H_c from the continuous film.

direction by head-on domain-wall motion. The reversal does not occur statistically independent in different stripes, but rather comprises several neighboring stripes, as was inferred from additional KM studies (not shown here), using a lower resolution. Each of the stripes still contains a multidomain state which is present even above H_c , as shown in Fig. 1(c). However, the amplitude of the magnetization modulation inside the stripes is strongly reduced.

From these observations we conclude that ripple domains and correlations in the multidomain ensemble play an essential role in the reversal process of the laterally patterned film. Ripple domains are well known from thin films. They are induced by irregular anisotropies connected with the polycrystalline structure of the film.¹¹ Indeed, in the continuous film the formation of ripple domains [see Fig. 1(d)] was observed. In patterned films ripple domains can be avoided if the shape anisotropy is large enough as was observed for 1.2- μm -wide stripes.⁸ But in the present case of 2.4- μm -wide stripes this is not the case and ripple domains occur.

The KM images in Fig. 1 already provide a good qualitative overview on the general features of the magnetization arrangement in the stripes and on the size distribution of the domains, ranging from several hundreds of nm to 1 μm in the parallel direction. However, they can hardly be used to obtain more quantitative information on the magnetization distribution within the domains at remanence and at higher fields. Neutron data provide the missing information by modeling the experimental results, using the direct-space KM images in Fig. 1 and MOKE measurements as input parameters.^{12,13} Figure 2 displays intensity maps taken by PNR as a function of the angle of incidence, α_i , and angle of exit, α_f . The maps are measured with (a) “spin-up” and (b) “spin-down” neutrons at a field well below $H_c \approx 100$ Oe applied parallel to the stripe direction [compare Fig. 1(a)] and with neutron polarization parallel or antiparallel to the field direction. The specular reflection ridge runs along the diagonal, where $\alpha_i = \alpha_f$. The Bragg diffraction is seen as curved off-specular lines at $\cos \alpha_i - \cos \alpha_f \approx n(\lambda/d)$, where n is the diffraction order. In Fig. 2, Bragg reflections for $n = \pm 1, \pm 2$ can be recognized. Note, that the diffraction effect is rather weak and visible only due to the neutron wave field enhancement close to the critical edges of total reflection for the incoming or the diffracted waves.¹⁵

The domain state of the stripes can be extracted in the intensity maps by two main effects: First, the intensity of the

specular and Bragg reflections is lowered [Figs. 2(a) and 2(b)] compared to results from maps measured in saturation (not shown). Second, and most important, the multidomain state causes a strongly asymmetric off-specular diffuse scattering, which is present at α_i and/or α_f close to the critical angles for total reflection. This effect is most pronounced at and below H_c , but can also be detected far above H_c and even close to saturation, when the magnetic contrast in KM is not sufficient enough to observe ripple domains. Off-specular magnetic scattering occurs only when the domains are smaller than the neutron coherence volume and when their magnetization vectors deviate from the mean magnetization direction within this coherence volume. The longitudinal coherence length (parallel to the neutron beam and perpendicular to the stripes) is estimated to be about 100 μm , while the transverse coherence length (parallel to the stripes) is only a few nm due to the focusing condition of the monochromator. The coherence volume, embracing a number of stripes in the lateral direction, is sketched in Fig. 3. In the following we will distinguish between the mean magnetization, which is the average taken by polarized neutron scattering within the coherence volume, and the net magnetization, which is the average taken over a large fraction of the sample and measured, for instance, via MOKE. While the net magnetization is parallel to the stripes, the mean magnetization is expected to deviate locally and show a large transverse and longitudinal distribution, as will be discussed in the following.

Between remanence and coercive field the mean magnetization manifests itself in Fig. 2 by the noticeable asymmetry in the off-specular scattering patterns. This asymmetry clearly signifies⁵ that locally the ripple magnetization deviates from the mean magnetization direction, while the mean magnetization has nonzero components parallel and perpendicular to the stripes. This is also confirmed by spin-flip specular intensity [as seen in Fig. 4(a) and discussed below] and off-specular Bragg reflections at $H \leq H_c$.

We have also taken reflectivity data with spin analysis of the exit beam, providing two cross sections for non-spin-flip (NSF), R^{++} and R^{--} , and two for spin-flip (SF), R^{+-} and R^{-+} , reflectivities. As shown in Fig. 4(a), above H_c we observe the typical ferromagnetic splitting between the two NSF reflectivities and almost no intensity for the SF reflectivities, $R^{+-} \approx R^{-+} \approx 0$. This unambiguously proves almost perfect alignment of the mean and the net magnetization. In the range $0 \leq H \leq H_c$, the splitting between R^{++} and R^{--} is lowered and SF occurs. The SF intensities indicate a magnetiza-

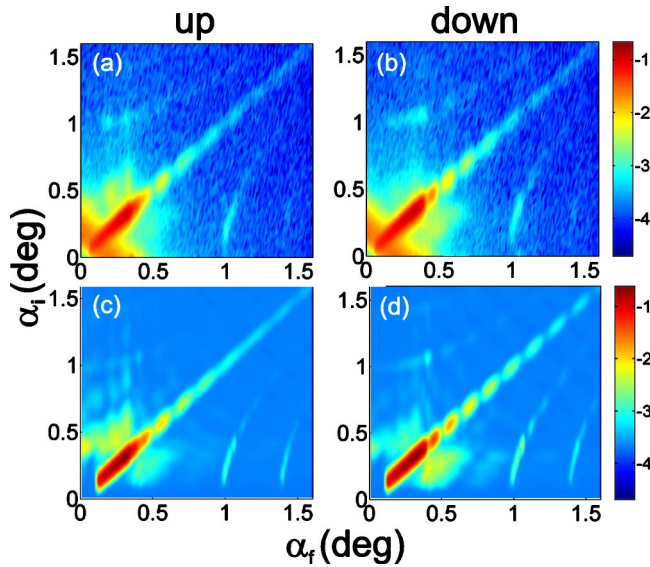


FIG. 2. (Color online) (a) and (b) experimental maps of the polarized neutron intensity on a logarithmic scale from a periodic stripe array measured at a magnetic field of 43 Oe and plotted as a function of the angles of incidence α_i , and the scattering angles α_f . (c) and (d) calculated intensity maps according to the domain model discussed in the text. (a) and (c) correspond to the incident neutron polarization parallel to the stripes and parallel to the external field, while in (b) and (d) the polarization and the field directions are antiparallel.

tion component perpendicular to the stripes which is very surprising for the easy-axis configuration. It occurs not only because of the existence of ripple domains. In fact, correlations between the ripples across the stripes are necessary to cause a nonvanishing transverse mean magnetization component over the coherence area (see below).

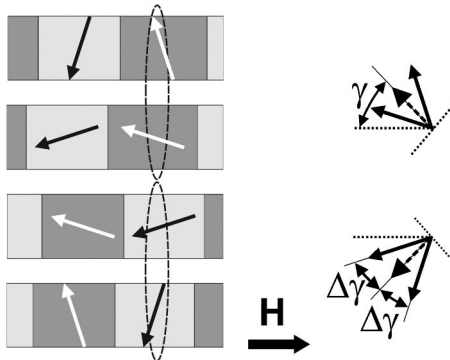


FIG. 3. Sketch for the model used in simulations. The dark and light gray shaded stripes represent the magnetic stripes with the ripple domains. The arrows indicate magnetization vectors within domains of individual stripes. The dashed line marks the neutron coherence volume, over which the average of the magnetization fluctuations are taken. For simplicity only two stripes within the coherence range are drawn, the actual size being much bigger. In the right part of the figure the dashed arrows indicate the mean magnetization direction averaged over a coherence volume. γ is the angle of the mean magnetization vector with respect to the stripe orientation. $\Delta\gamma$ is the transverse fluctuation about the mean value. For further details see text.

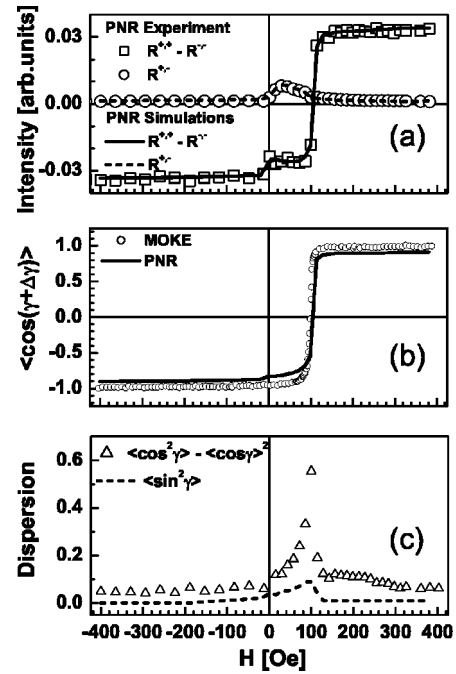


FIG. 4. (a) Splitting $R^{++}-R^{--}$ between non-spin-flip and spin-flip $R^{+-}=R^{-+}$ reflectivities as a function of applied field; (b) field dependence of the mean projection of the normalized magnetization onto the easy axis as determined from MOKE (circles) and PNR (line) data; (c) field dependence of the longitudinal dispersion $\langle\cos^2\gamma\rangle-\langle\cos\gamma\rangle^2$ of the domain magnetization vectors (open triangles), and transverse dispersion $s_\gamma^2=\langle\sin^2\gamma\rangle$ (dashed line).

The model calculations of the intensity maps shown in Figs. 2(c) and 2(d) are based on the domain state model in Fig. 3 and have been calculated using the distorted-wave Born approximation (DWBA).^{12,13} It is assumed that domains within a stripe are separated by $\sim 90^\circ$ -type walls, running the shortest distance across the stripes. The magnetization vectors within the domains, indicated by arrows, are tilted at angles $\gamma\pm\Delta\gamma$ with respect to the net magnetization directed along the stripe axis. This configuration unavoidably leads to leakage of magnetic flux into the inter-stripe region which energetically is unfavorable. This is, however, compensated by the gain in dipolar energy due to the head-to-tail orientation of their perpendicular magnetization components in neighboring stripes. The mean magnetization direction, denoted by the dashed ellipse in Fig. 3, is $\gamma_{\text{coh}}=\langle\gamma\pm\Delta\gamma\rangle_{\text{coh}}\neq 0$.

Next we consider the projection of the mean magnetization parallel and perpendicular to the stripes. Because of fluctuations $\Delta\gamma$, the mean value is given by $\langle\cos(\gamma\pm\Delta\gamma)\rangle_{\text{coh}}=c_\Delta c_\gamma\leq c_\gamma$, where $c_\gamma=\langle\cos\gamma\rangle_{\text{coh}}$, $c_\Delta=\langle\cos\Delta\gamma\rangle_{\text{coh}}\leq 1$, at $\langle\sin\Delta\gamma\rangle_{\text{coh}}=0$. At the same time the mean perpendicular magnetization component averaged over the coherence area, $\langle\sin(\gamma\pm\Delta\gamma)\rangle_{\text{coh}}=c_\Delta\langle\sin\gamma\rangle\neq 0$, does not vanish. It vanishes, however, after averaging over the whole sample. This is not the case for $s_\gamma^2=\langle\sin^2\gamma\rangle\neq 0$, which causes SF specular reflection.

The complete set of reflectivities, R^{++} , R^{--} , R^{+-} , R^{-+} , was fitted by varying three parameters, c_Δ , c_γ and s_γ^2 under the constraint $\langle\cos\gamma\rangle^2\leq\langle\cos^2\gamma\rangle=1-s_\gamma^2$. In Fig. 4(a), the solid

lines reproduce the simulations and the symbols are the experimental data points. The agreement between experiment and theory is excellent. Figure 4(b) compares the mean value $\langle \cos(\gamma \pm \Delta\gamma) \rangle$ from MOKE measurements (solid line) with those deduced from PNR by the product $c_{\Delta}c_{\gamma}$. The PNR results show slightly lower absolute values of $\langle \cos(\gamma \pm \Delta\gamma) \rangle$, the difference being due to the sensitivity of PNR to the magnetic inductance, which has contributions within and in between the stripes. In Fig. 4(c), we have plotted the longitudinal mean-square fluctuations of the domain magnetization vectors, $\langle \cos^2 \gamma \rangle - \langle \cos \gamma \rangle^2$, and the mean-square transverse magnetization component s_{γ}^2 . They both peak at the coercive field H_c , where the fluctuations are largest.

Finally, we discuss the origin of the off-specular and asymmetric diffuse magnetic scattering as seen in the maps of Fig. 2. The diffuse scattering stems only from the coherence volume, where the effects of longitudinal and transverse fluctuations of the mean magnetization are preserved. Due to randomness $\langle \sin \Delta\gamma \rangle_{\text{coh}} = 0$, only the transverse dispersion averaged over the coherence range, $s_{\Delta}^2 = \langle \sin^2 \Delta\gamma \rangle_{\text{coh}} \neq 0$, provides off-specular SF scattering, while the longitudinal dispersion, $c_{\Delta}^2 = \langle \cos^2 \Delta\gamma \rangle_{\text{coh}} - \langle \cos \Delta\gamma \rangle_{\text{coh}}^2$, contributes to off-specular NSF scattering. Furthermore, the fluctuations $\Delta\gamma$ are found to be correlated over distances of at least $\xi = 20 \mu\text{m}$ across the stripes. A set of parameters for the remanent state, $c_{\gamma} = -0.89$, $s_{\gamma}^2 = 0.05$, $c_{\Delta} = 0.9$, and $s_{\Delta}^2 = 0.19$, allows not only to reproduce the basic features of data, as shown in Figs. 2(c) and 2(d), but also to correctly describe

the ratio between specular reflected, diffracted, and scattered intensity. From this we infer that the individual domain magnetization directions slightly fluctuate about the mean value. The mean value itself is tilted by almost $\pm 30^\circ$ with respect to the stripes at 43 Oe before switching, which corresponds to the magnetization of the ripple domains observed with KM.

In summary, we have shown that polarized specular and off-specular neutron scattering provides a detailed picture of the mean domain magnetization vectors in a magnetic stripe array, including longitudinal and transverse fluctuations about the mean magnetization and correlation effects between magnetic domains across different stripes. As a result of a quantitative analysis we have found that the domain magnetization vectors are heavily correlated not only parallel to the stripe direction, but also over a large perpendicular distance between them, a phenomenon which has not been described for the case that the field reversal and the main magnetization direction are parallel to the field direction. This correlation creates an inherent instability of the system with respect to the formation of large domains as observed during the magnetization reversal.

This study has been financially supported by the DFG (SFB 491) and by BMBF O3ZA6BC1. We thank M. Wolff for experimental help at the ADAM reflectometer. B.P.T. thanks the DFG for financial support.

*Electronic address: k.theis-broehl@rub.de

[†]On leave from Petersburg Nuclear Physics Institute, 188300, Gatchina, Russia.

¹M. R. Fitzsimmons, P. Yashar, C. Leighton, I. K. Schuller, J. Nogues, C. F. Majkrzak, and J. A. Dura, *Phys. Rev. Lett.* **84**, 3986 (2000).

²M. Gierlings, M. J. Prandolini, H. Fritzsche, M. Gruyters, and D. Riegel, *Phys. Rev. B* **65**, 092407 (2002).

³S. G. E. te Velthuis, G. P. Felcher, S. Jiang, A. Inomata, C. S. Nelson, A. Berger, and S. D. Bader, *Appl. Phys. Lett.* **75**, 4174 (1999).

⁴W. T. Lee, S. G. E. te Velthuis, G. P. Felcher, F. Klose, T. Gredig, and E. D. Dahlberg, *Phys. Rev. B* **65**, 224417 (2002).

⁵V. Lauter-Pasyuk, H. J. Lauter, B. P. Toperverg, L. Romashev, and V. Ustinov, *Phys. Rev. Lett.* **89**, 167203 (2002).

⁶J. A. Borchers, J. A. Dura, J. Unguris, D. Tulchinsky, M. H. Kelley, C. F. Majkrzak, S. Y. Hsu, R. Loloee, W. P. Pratt, and J. Bass, *Phys. Rev. Lett.* **82**, 2796 (1999).

⁷K. Temst, M. J. Van-Bael, and H. Fritzsche, *Appl. Phys. Lett.* **79**, 991 (2001); H. Fritzsche, K. Temst, M. J. Van-Bael, V. V. Mosh-

chalkov, Y. Bruynseraede, H. Fritzsche, and R. Jonckheere, *Appl. Phys. A: Mater. Sci. Process.* **74**, S1538 (2002).

⁸K. Theis-Bröhl, T. Schmitte, V. Leiner, H. Zabel, K. Rott, H. Brückl, and J. McCord, *Phys. Rev. B* **67**, 184415 (2003).

⁹W.-T. Lee, F. Klose, H. Q. Yin, and B. P. Toperverg, *Physica B* **335**, 77 (2003).

¹⁰A. Schreyer, R. Siebrecht, U. Englisch, U. Pietsch, and H. Zabel, *Physica B* **248**, 349 (1998).

¹¹A. Hubert and R. Schäfer, *Magnetic Domains* (Springer, Heidelberg, 1998).

¹²S. K. Sinha, E. B. Sirota, S. Garoff, and H. B. Stanley, *Phys. Rev. B* **38**, 2297 (1988).

¹³B. P. Toperverg, *Physica B* **297**, 160 (2001); *Appl. Phys. A: Mater. Sci. Process.* **74**, S1560 (2002); B. P. Toperverg, in *Polarized Neutron Scattering*, Matter and Materials Series Vol. 12, edited by Th. Brückel and W. Schweika (Schriften des Forschungszentrum, Jülich, 2002), p. 249.

¹⁴Mean and net magnetizations are defined in the text below.

¹⁵The direct beam shows up in the left bottom corners of the intensity maps.